Nano Plus: Sci. Technol. Nanomater. 4 (2022) 57–66

https://doi.org/10.48187/stnanomat.2022.4.007

Nano Plus: Science and Technology of Nanomaterials
Journal home page: https://www.stnanojournal.org/
ISSN: 2782-8166 (print) 2782-8174 (electronic)

Corrosion inhibition performance of silver nanoparticles embedded-gloss paint on carbon steel and aluminium substrates in 2.0 M H_2SO_4 solution

[1]Asafa T. B., [2*]Olawore A. S., [3]Odusote J. K., [3]Enone G. A., [1]Lateef A. and [4]Adeleke A. A.

[1]Nanotechnology Research Group, Ladoke Akintola University of Technology Ogbomoso, Nigeria.
[2]Department of Mechanical Engineering, Kwara State University Malete, Ilorin, Nigeria.
[3]Department of Materials and Metallurgical Engineering, University of Ilorin, Ilorin, Nigeria.
[4]Department of Mechanical Engineering, Nile University, Abuja, Nigeria.

Article info

Received: May 24, 2022
Revised: Jun. 28, 2022
Accepted: Jun. 30, 2022

Keywords:
AgNPs,
Mild steel,
Gravimetric,
Potentiodynamic polarization,
Gasometric,
Corrosion control

Abstract

Corrosion control of metals in aggressive environments has attracted a lot of attention due to its associated economic losses. However, most corrosion control techniques have not satisfactorily minimized these losses. This study examined the inhibition effects of silver nanoparticles (AgNPs) incorporated in gloss paint on corrosion of carbon steel and aluminium in 2.0 M H_2SO_4 solution. The AgNPs were biosynthesised via green chemistry and characterized using Fourier Transform Infrared, UV-Vis spectrometer, and Transmission Electron Microscope. Samples of carbon steel and aluminium were uniformly coated with a thin layer of gloss paint mixed with AgNPs solution at five different concentrations of 0, 5, 10, 15, and 20 µg/ml. The inhibition efficiency of the AgNPs modified paint was conducted via gravimetric, gasometric, and potentiodynamic polarization analyses. Results of the gravimetric analysis revealed an increased weight loss with an increased period of exposure and decreased concentration of AgNPs in the paint. The corrosion rates for the mild steel and aluminium samples were 0.051 and 0.005 mm with inhibition efficiencies of 42% and 69%, respectively, when immersed in 20 µg/ml AgNPs-incorporated coating and exposed for 120 hours. Potentiodynamic polarization analysis revealed that the presence of AgNPs in the paint (as inhibitor) retarded the anodic dissolution by the formation of protective films on the mild steel and aluminium sample surfaces. The evolution of hydrogen gas from 20 µg/ml AgNPs-incorporated coating was significantly reduced by 81% and 14% for mild steel and aluminium, respectively, when compared with the control samples at 200 mins of exposure. These results revealed that incorporation of AgNPs into the gloss paint matrix minimizes the degradation due to corrosion of the mild steel and aluminium samples.

1. Introduction

Carbon steel and aluminium are two commonly used metals in industries. Carbon steel is used in machinery parts, steel frame buildings, cookware, and pipelines, among others. Aluminium find applications in construction, power lines, aircraft, as well as precision tubing. These engineering materials are indispensable due to their unique properties such as strength, toughness, ductility, thermal and electrical conductivity, weldability among others [1]. However, the properties are degraded when exposed to corrosive environments leading to loss or contamination of products, decrease in efficiency, destruction of valuable resources, expensive maintenance and global economic losses amounting to billions of dollars annually [2].

Acidic media such as sulfuric and hydrochloric acid have violent corrosive effects on the surfaces of exposed metals. Sulfuric acid is one of the most important acidic solutions that

Corresponding authors: ayodeji.olawore@kwasu.edu.ng

are widely applied for the removal of scales and unwanted dust from the metal surface prior to electroplating or coating. It is also applicable in oil-well acidizing, acid pickling, and industrial cleaning [3–5]. This consequently makes the metals vulnerable and prone to corrosion during industrial application. The corrosive effects on the metallic surfaces can be minimized or controlled by using different approaches such as protective coating [6], alloying [7, 8], cathodic protection [9, 10], use of inhibitors [11, 12], heat treatment [13], and environmental modifications [14].

Corrosion inhibitors are needed to protect metal surfaces from corrosion when exposed to acidic media. The efficacy of the inhibitor depends on the structural characteristics of the inhibitor, the types of the corrosive environment, and the types of the metal surface and electrochemical potential at the interface [15]. Corrosion inhibitors can adsorb or form a thin film of passive layer on the metallic surface and react with corrosion products to form insoluble complexes that appreciably impede the corrosion substances from permeating through the metal substrates [16]. However, the corrosion inhibitor may hydrolyze and disintegrate during the corrosion reaction process. Hence, this process would lead to a large amount of inhibitor at the beginning of the corrosion reaction to a lower amount of the inhibitor at the end [1]. Corrosion inhibitors can be classified into three categories namely; organic inhibitors, inorganic inhibitors, and mixed material inhibitors [5, 17–19].

Organic inhibition is synthetic and not environmentally friendly because toxic products are released into the ecosystem once used. This has consequently diverted the attention of researchers to eco-friendly inhibitors that are safe, biodegradable, non-toxic, and readily available [20]. Thus, promising results have been attained using plant extracts to synthesize nanoparticles for improved inhibition efficiency and eco-friendliness. The nanoparticles synthesized by the green approach have exhibited low toxicity with varied shapes and sizes [11, 12, 21 - 26]. Further studies have shown that silver nanoparticles (AgNPs) are a promising corrosion resistance agent by providing a protective coating on a metallic surface. The incorporation of AgNPs into hydrochloric acid medium enhanced the inhibition efficiency for mild steel, stainless steel, and aluminium [12, 20, 24].

The corrosive effects on the metallic surfaces can also be minimized by applying a protective coating. Gloss paint is frequently used because it creates a beautiful, long-lasting, and lustrous finish. The paint is made up of a binder (alkyd resin), pigment, solvent, and additive. An aliphatic petroleum solvent is used to dissolve the resin, making it easier to disperse. When the solvent evaporates, the oxygen in the air reacts with the resin, resulting in the development of cross-links between the polymer molecules and the production of a thick, dry film that prevents water and oxygen from entering and corroding the metal [32]. These protective barrier coatings have chemical or physical properties that inhibit corrosion reactivity and/or material deterioration caused by external influences such as weathering, blistering, and fouling. However, silver nanoparticles have a stronger reactivity to an aqueous acidic solution [16]. AgNPs have been deployed as additives to improve the anti-corrosion properties of coatings [27]. In order to improve the anti-corrosion properties of gloss paint, the corrosion performance of gloss paint incorporated with AgNPs in an acidic medium would be examined to determine the efficacy of the coating matrix.

This study reported the use of AgNPs biofabricated from Cola nitida and incorporated in gloss paint as a corrosion inhibitor of carbon steel and aluminium in 2.0 M H_2SO_4 solution. inhibition performance was evaluated using weight loss measurement, potentiodynamic polarization measurement (PPM), and gasometric analysis.

https://doi.org/10.48187/stnanomat.2022.4.007

2. Materials and methods

2.1 Preparation of AgNPs

The details of the synthesis and characterization of AgNPs employed in this research are published elsewhere by Lateef et al. [26], but the synopsis of the process is provided here. AgNPs were prepared from silver salts by using Cola nitida pod extract as the reducing agent. The characterization was done using FTIR, TEM, selected area electron diffraction (SAED) and UV–Vis.

2.2 Preparation of the metal substrates

Two metals, carbon steel and aluminium, were used. Their elemental compositions were determined using an optical light emission spectrometer (QualiSpark 750) and positive materials identification (PMI) machine (X-MET8000 Series), respectively. The metal samples were cut into dimensions of 20 mm by 25 mm each with a hole of 1mm diameter to enable easy suspension and removal of the metal samples in and out of the corrosive medium. The carbon steel and aluminium samples were then polished sequentially with emery papers of different grades of 120, 220, and 320 grit and degreased in ethanol. The polished metal samples were subsequently cleaned with acetone. They were dried and kept in a desiccator to prevent moisture from coming in contact with the sample following the technique used elsewhere [28].

2.3 Preparation of the coated substrates and corrosive environment

Silver nanoparticles solution at different concentrations of 5 µg/ml, 10 µg/ml, 15 µg/ml, and 20 µg/ml were prepared by diluting 180 µg/ml of AgNPs solution with 175 ml, 85 ml, 55 ml, and 40 ml volume of deionized water respectively. The concentrations were further mixed with the gloss paint in five different containers. The silver nanoparticles of 20 ml each with the concentration of 5 µg/ml, 10 µg/ml, 15 µg/ml, and 20 µg/ml were mixed with 80ml of the gloss paint. These mixtures were stirred uniformly to prevent the agglomeration of AgNPs. The metal samples were then uniformly coated with a mixture of gloss paint and silver nanoparticles by using Spraygun (DeVilbiss FLG5). The samples were subsequently dried and cured. The control paint did not contain AgNPs solution. The coated metals (with or without AgNPs)

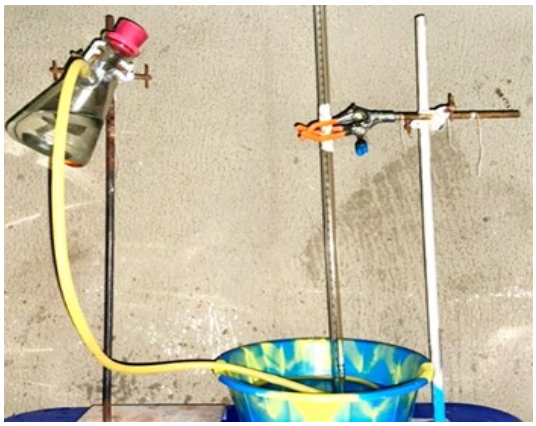

Fig. 1: Gasometric analysis setup

were completely immersed in a 2.0 M H_2SO_4 corrosive environment for further analysis as discussed in subsequent subsections.

2.4 Corrosion measurement approaches

The inhibition efficiency of the coated metals in the corrosive medium was then analyzed using weight loss, potentiodynamic polarization, and hydrogen gas evolution techniques.

2.4.1 Gravimetric analysis

The coated metals (with or without AgNPs) were completely immersed in 200 mL of 2.0 M H_2SO_4. Samples were weighed with a digital weighing balance of ± 0.01g sensitivity before immersion. They were withdrawn after 24, 48, 72, 96, and 120 hours of exposure to the solution, cleaned with ethanol, and dried at room temperature. The samples were weighed again to estimate the weight loss due to exposure to the acidic solution.

The Corrosion rate (CR) and inhibition efficiency (IE) were evaluated using Eqn (1) and (2), respectively.

https://doi.org/10.48187/stnanomat.2022.4.007

$$CR = \frac{8.76\Delta W}{\rho AT} \quad \ldots (1)$$

$$IE\% = \frac{W_o - W}{W_o} \times 100 \quad \ldots (2)$$

Where A is the surface area of the metal sample (cm^2), T is the exposure time (hr), ρ is the density of the metal (g/cm^3), ΔW is the weight loss (g), and W_o and W are the weights of the metal samples before and after immersion respectively.

2.4.2 Potentiodynamic Polarization (PP) Measurement

Potentiodynamic polarization measurement was conducted using the AUTOLAB PGSTAT 101 instrument. The metal samples with a surface area of 100 mm^2 were embedded in resin at room temperature and then polished with different grades of emery papers until a shiny smooth surface was accomplished. The working electrode, which was the metal samples, was dipped together with the counter electrode and the reference electrode into a beaker containing 200 ml of 2.0 M of H_2SO_4 serving as the electrolyte. Furthermore, the open-circuit corrosion potential was conducted for 30 minutes until a stable potential was achieved. The test was carried out from a cathodic potential of -250 mV to an anodic potential of +250 mV with a scan rate of 1.0 mVs^{-1}. The surface coverage (θ) and inhibitor efficiency (IE %) were determined using Equations (3) and (4), respectively.

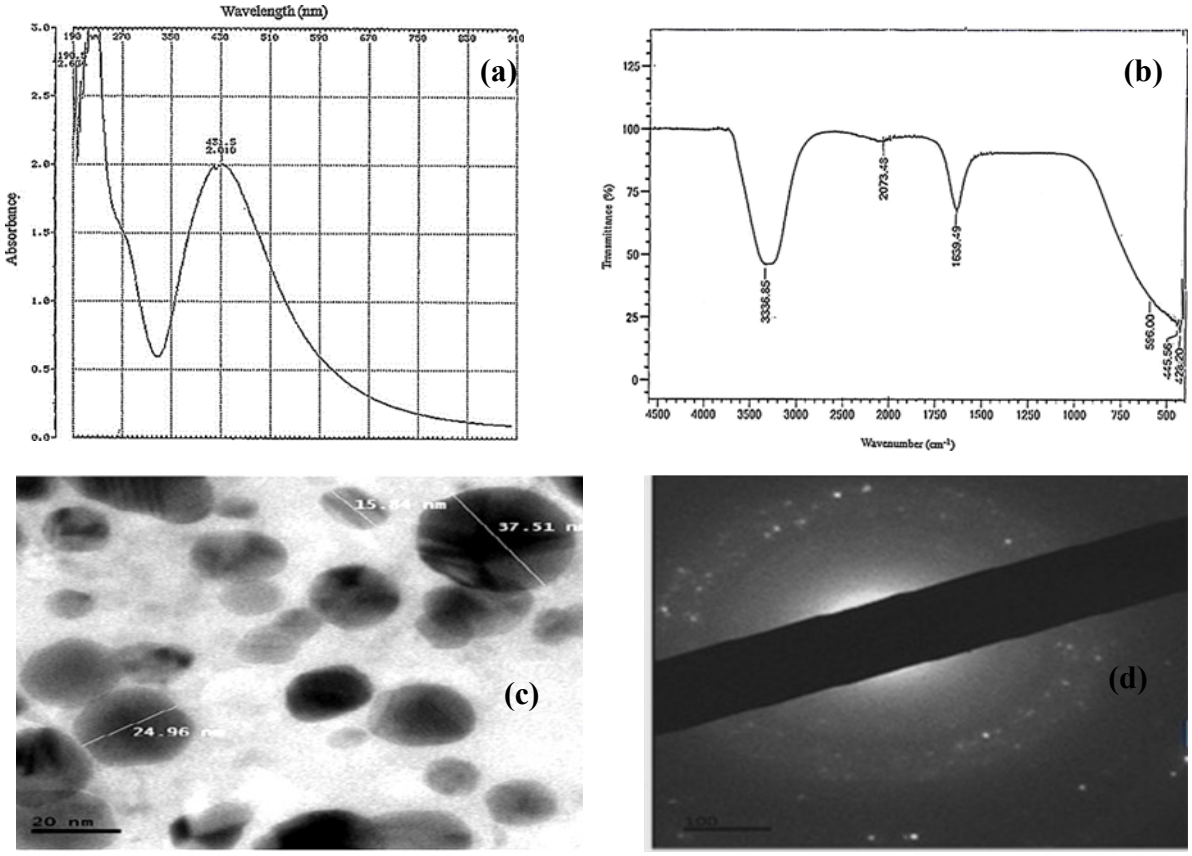

Fig. 2: (a) UV–vis spectrum (b) FITR spectrum (c) Transmission electron micrograph and (d) selected area electron diffraction pattern of the synthesized AgNPs [26].

$$\theta = \frac{I_{corr} - I_{*corr}}{I_{corr}} \quad \ldots (3)$$

$$IE\% = \frac{I_{corr} - I_{*corr}}{I_{corr}} \times 100 \quad \ldots (4)$$

Where I_{corr} and I_{*corr} are corrosion current densities in the absence and presence of the inhibitor.

https://doi.org/10.48187/stnanomat.2022.4.007

2.4.3 Gasometric Analysis

Hydrogen evolution measurements were conducted using a Buckner flask, burette, pipette, cork (to prevent the escape of the hydrogen gas), and a tiny hose as shown in Figure 1. The weighed test specimens were completely immersed in H_2SO_4 medium. The flask was closed immediately by using the cork to thwart the escape of gases and guarantee the flask was airtight. The resulting volume of hydrogen gas generated during the corrosion reaction was observed via the downward movement of water. The volume of hydrogen evolution was measured against the exposure time for all samples in 2.0M H_2SO_4 at 20 minutes intervals for 200 minutes.

3. Results and Discussion

3.1 Characteristics of AgNPs

The biosynthesized nanoparticles exhibited the highest absorbance at a wavelength of 431.5 nm as shown in Figure 2a. Moreover, the FTIR results revealed strong peaks at 3336.85, 2073.48, and 1639.49 cm^{-1} as seen in Figure 2b which confirmed that the synthesized AgNPs were stabilized by proteins. The size of the synthesized AgNPs was within the range of 5-40 nm with spherical shapes (Figure 2c). The nanoparticles were crystalline with distinguishing ring-like selected area electron diffraction (SAED) patterns (Figure 2d) [26].

3.2 Elemental compositions of the carbon steel and aluminium

The compositions of the carbon steel and aluminium samples are shown in Table 1 and Table 2, respectively. Table 1 indicates that the steel sample contains very low carbon content (0.011%) which invariably means that the steel belongs to the class of low carbon steel with standard designation of AISI 1010 [33]. According to Table 2, the aluminium sample belongs to the 1xxx series because of the minimal trace elements [34].

3.3 Weight loss analysis

The weight losses for all the samples tested versus time are shown in Figure 3. There was a decrease in weight loss as the concentration of the AgNP-inhibited coating on the metal surface increased compared to that of the control sample. This is due to the excellent adhesion of the AgNP-inhibited coating on the metallic surface which invariably created a protective film on the substrates. These protective films serve as the barrier between the metallic substrate and the aggressive acidic environment which consequently prevents reaction between the metallic surface and the sulphuric acid. The existence of AgNPs in the coating improved the development of passive layers on the metallic surface and thereby enhance the inhibition efficiency. This functionality may be due to the existence of crude protein, alkaloids, caffeine, theobromine, nicotine, and kolatine present in the nanoparticles [29].

Table 1: Elemental composition of carbon steel sample in wt%

Element	C	Si	Fe	Cr	Mn	P	Al	S	Cu	Ni	Co
Weight	0.011	0.001	99.7	0.034	0.102	0.022	0.013	0.005	0.014	0.002	0.016

Table 2: Elemental composition of aluminium sample in wt%

Element	Zn	Si	Fe	Mn	Pb	Al	Cu	Ni
Weight	0.025	0.524	0.539	0.013	0.001	98.829	0.062	0.006

The weight loss for mild steel and aluminium samples coated without AgNPs solution (control samples) after 120 hrs of exposure is 3.45 mg and 0.19 mg, respectively. The weight loss was reduced to 3.05mg and 0.16mg, respectively with 5µg/ml AgNP-inhibited coating. The weight loss for the mild steel and aluminium further decreased to 2.76

https://doi.org/10.48187/stnanomat.2022.4.007

mg and 0.09 mg respectively when 20 µg/ml AgNP was added to the gloss paint. These results indicate that the weight loss in mild steel and aluminium reduced with increased concentration of the AgNPs (inhibitor) [12].

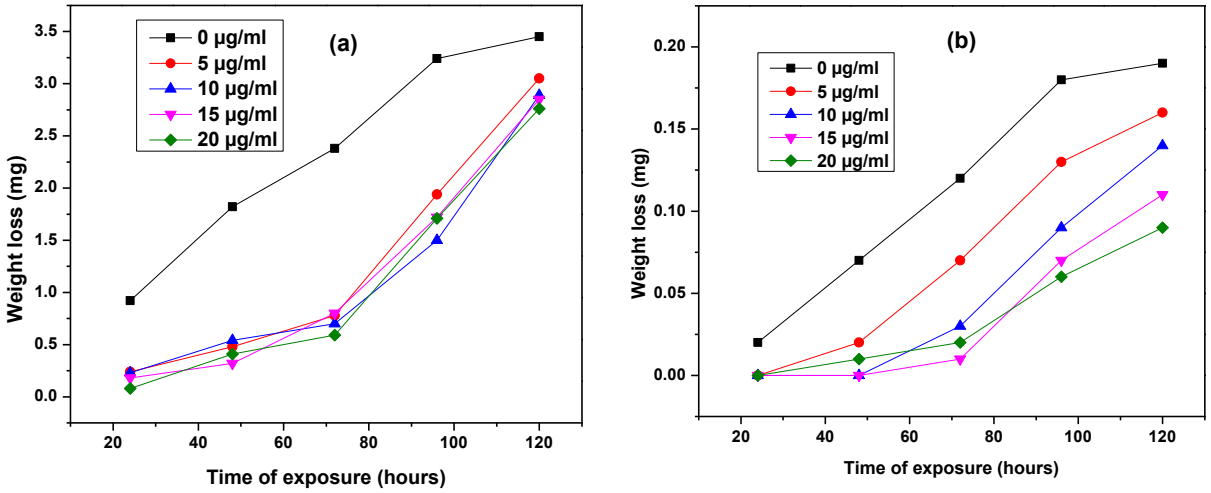

Fig. 3: Weight loss for (a) mild steel (b) aluminium against the time of exposure with and without inhibitor in 2 M H_2S0_4

The firmness of the inhibition performance of the extract was estimated in terms of inhibition efficiency (IE) which depends on the period of exposure (Figure 4). The inhibition efficiency of the AgNPs-embedded coating on the mild steel and aluminium substrates was improved by 42% and 69%, respectively. The inhibition efficiency increased as the concentration of the AgNP-inhibited coating and period of exposure to the acidic medium increased which is similar to the findings of a previous study [12]. This observation can be attributed to the excellent adherence of the AgNP-inhibited coating to the metal surface and the consequent formation of protective film acting as a barrier between the metal and the corrosive environment. Although, the addition of nanoparticles minimizes the dissolution of metallic ions; however, it is not adequate to fully impede the reactive surface of the metal alloys from the acidic medium [11]. Consequently, AgNPs could act as a feasible inhibitor for metal alloys in the H_2SO_4 medium.

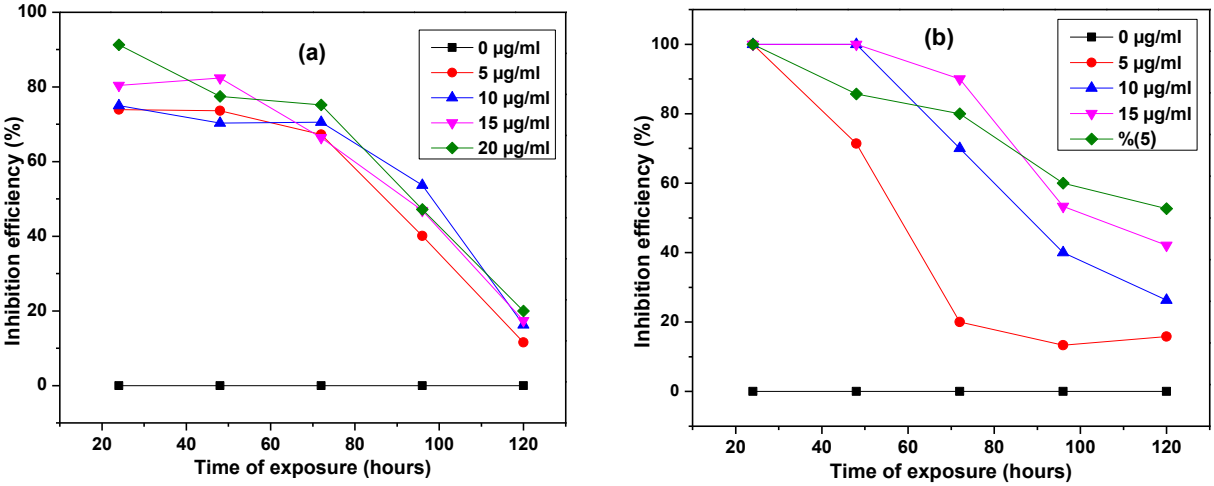

Fig. 4: The inhibition efficiency of (a) mild steel (b) aluminium against the time of exposure with and without inhibitor in 2 M H_2S0_4

The rate of corrosion of carbon steel and

https://doi.org/10.48187/stnanomat.2022.4.007

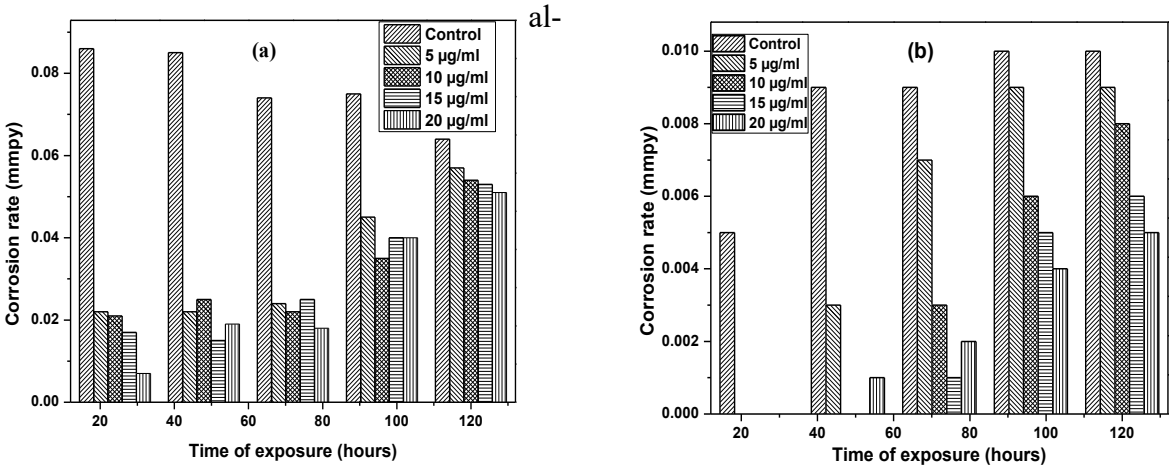

Fig. 5: The corrosion rate of (a) mild steel and (b) aluminium versus the time of exposure with and without inhibitor in 2.0 M H_2SO_4.

uminium decreased as the concentration of AgNP-inhibited coating increased (Figure 5). Mild steel samples, on average, have one order of magnitude of corrosion rate higher than aluminium samples. For instance, the corrosion rate for mild steel and aluminium with 20µg/ml AgNP-inhibited coating exposed for 120 hours were 0.051 and 0.005 mmpy, respectively. Though, the surfaces are completely protected by the inhibition film that formed a passive layer on the surface of the samples which leads to optimal inhibition efficiency in 2.0 M H_2SO_4 solution. This result conforms with the finding of previous researchers [11].

3.4 Potentiodynamic polarization study

The potentiodynamic polarization curves for the corrosion experiments are depicted in Figure 6. The anodic Tafel slope (βa) and cathodic Tafel slope (βc) were obtained by extending the linear segments of the respective curves to the corrosion potential axis. The point at which the anodic Tafel line and the cathodic Tafel line meet produced the corrosion current density (Icorr) and corrosion potential (Ecorr) along the horizontal and vertical axes, respectively. The corrosion parameters based on the potentiodynamic polarization study are provided in Table 3. The corrosion current density (Icorr) decreased as the concentration of the inhibitors increased due to sufficient adhesion of the inhibitor occasioned by the AgNPs embedded in the paint. Consequently, the rate of electrochemical reactions was minimized. The inhibitor is said to act as a cathodic or anodic type inhibitor for either carbon steel or aluminum because of the displacement of more than 85 mV from the Ecorr values compared to that of the control samples. It retards both the cathodic and anodic reactions, but it is more effective on the cathodic reactions. Thus, the inhibitor serves as a cathodic inhibitor for carbon steel and aluminium [30]. The inhibition effect and the polarization resistance also increased with increased concentration of AgNPs. This implies a decrease in the rate of corrosion of carbon steel and aluminium which conforms with previous findings [12].

3.5 Hydrogen evolution measurement

The volume of hydrogen gas evolution increased with time of exposure (Figure 7) which was more rapid in the control steel sample than in the aluminium sample due to the aggressive attack of H_2SO_4 on the steel. However, a protective layer of Fe_2SO_4 was formed on the mild steel leading to a reduction in the hydrogen evolution (see Equation 5) [31].

$$H_2SO_4 + Fe \rightarrow FeSO_4 + H_2 \quad \ldots (5)$$

However, when nanoparticles were introduced, the volume of hydrogen gas produced

https://doi.org/10.48187/stnanomat.2022.4.007

Table 3: Potentiodynamic polarization parameters for samples with and without silver nanoparticles for mild steel and aluminium exposed in 2M H_2SO_4 solution.

Metal	Conc. (µg/ml)	E_{corr} (mV)	I_{corr} (mA)	βa (mV/dec)	βc (mV/dec)	C.R (mmpy)	Surface coverage	IE (%)
Mild steel	0	-720.97	1.4854	-171.98	79.676	17.26	0	0
	5	-885.97	0.0014	96.29	280.820	0.017	0.99	99.90
	10	-835.34	0.0010	43.10	16.693	0.012	0.99	99.93
	15	-891.75	0.0015	51.52	19.492	0.018	0.99	99.90
	20	-745.33	0.0206	55.85	76.514	0.239	0.98	98.61
Aluminium	0	-935.18	0.1040	113.00	-336.630	1.209	0	0
	5	-1119.20	0.0059	154.02	337.070	0.068	0.94	94.34
	10	-1064.20	0.0002	58.90	86.512	0.003	0.99	99.79
	15	-1051.00	0.0014	43.58	83.886	0.016	0.98	98.70
	20	-943.51	0.0013	30.52	22.534	0.015	0.98	98.75

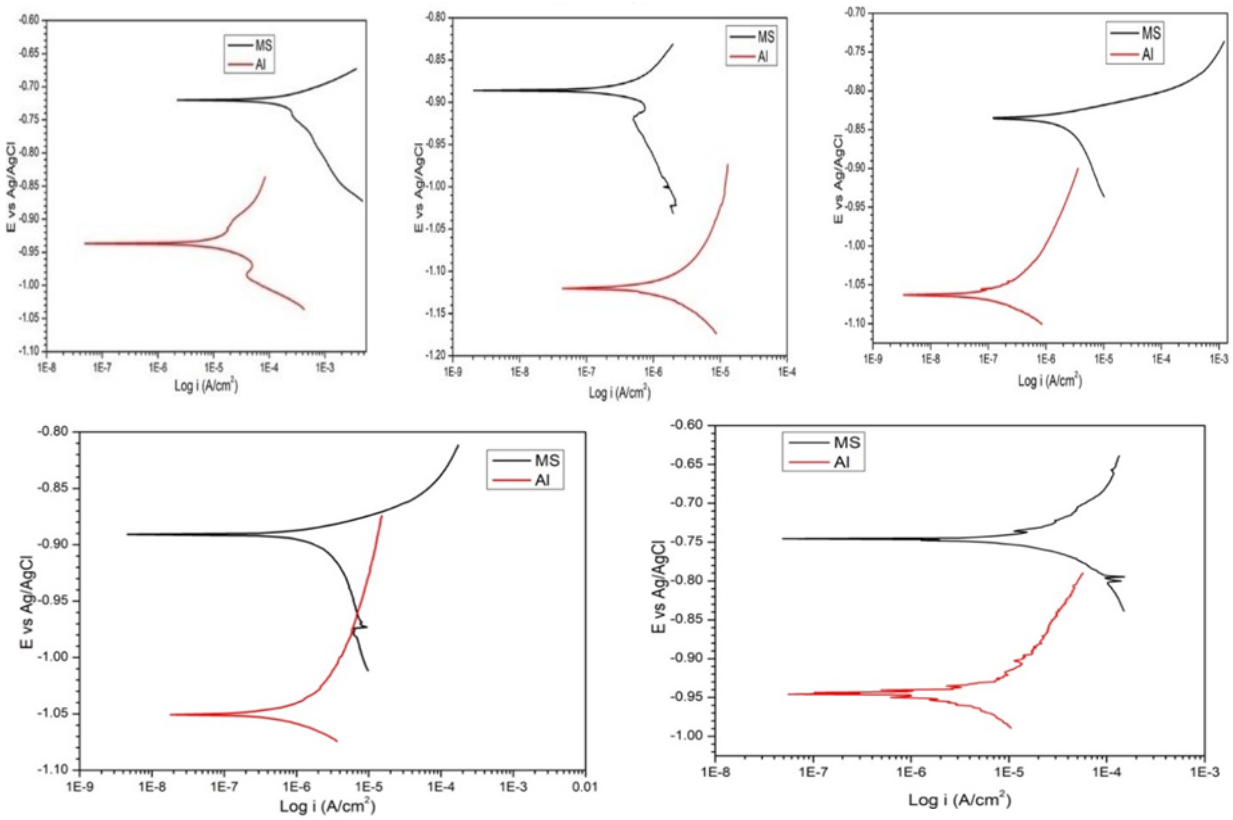

Fig. 10: Variation of collector efficiency for different working fluids with Reynolds number

reduced compared to the control sample which conforms with a previous study [28]. This observation is adduced to the proper adhesion of the nanoparticle embedded paint coating on the surface of the mild steel which consequently led to surface passivation and the formation of protective film acting between the metal and the aggressive acidic environment. Thus, the rate of metal dissolution is reduced and impeded.

The slow rate of hydrogen evolution for the aluminium control sample was attributed

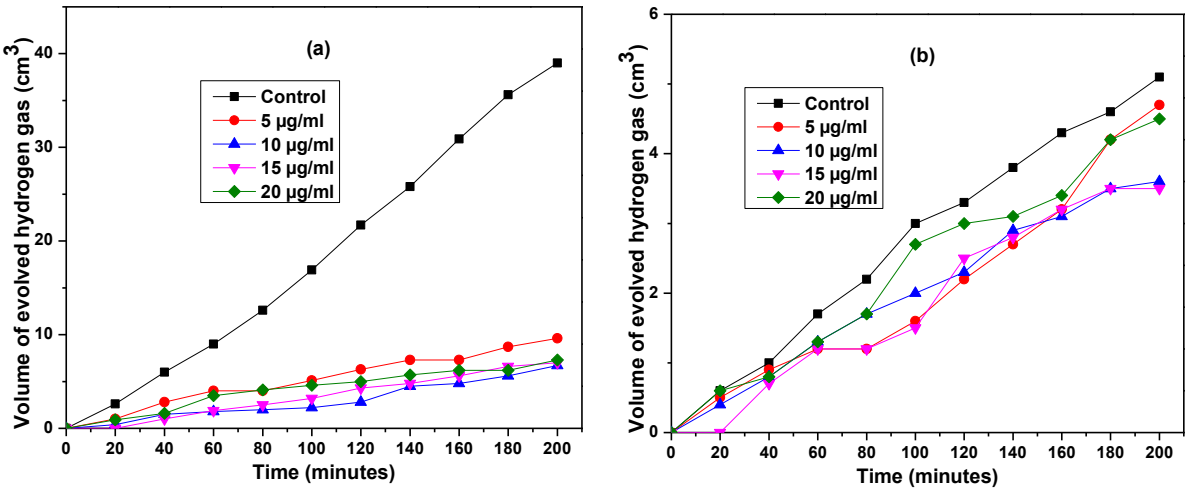

Fig. 7: The volume of hydrogen gas evolution of (a) mild steel and (b) aluminium samples against the time of exposure at varying concentrations in 2 M H_2S0_4.

to the excellent corrosion resistance of the aluminium, and the formation of aluminium oxide when placed in an oxidizing environment. Also, the higher concentration of AgNPs resulted in a decrease in the evolution of hydrogen gas (Figure 7b). The strong adhesion between the nanoparticles-modified paint and the metals led to the surface passivation that acts as a barrier layer between the metal and the H_2SO_4 solution. The evolution of hydrogen gas of AgNP-inhibited coating at a concentration of 20µg/ml was reduced by 81% and 14% for mild steel and aluminium, respectively when compared with their respective control samples at 200 mins of exposure. The suitability of nanoparticles as an inhibitor of carbon steel and aluminium corrosion in an acidic environment can be affirmed due to the good inhibition characteristics exhibited by AgNPs on the samples.

4. Conclusion

The AgNPs produced via biogenic synthesis of *Cola nitida* pod can be applied in coating industries to improve the inhibition of mild steel and aluminum in a 2M H_2SO_4 medium. The results of AgNP-inhibited coating on the metallic substrates obtained from weight loss, potentiodynamic polarization, and geometric analysis revealed that the existence of AgNPs as the inhibitor in the coating matrix retarded the anodic dissolution by the formation of protective films or layers on the metallic surfaces. This occurred due to surface passivation with the protective film that acted as the barrier between the metal and the aggressive acidic environment of 2M H_2SO_4. Thus, the rate of metal dissolution was retarded. However, the evolution of hydrogen gas of AgNP-inhibited coating was limited to 200 mins of exposure in this study. The protective film deteriorates during the evolution of hydrogen, and this will result in increases in the rate of metal dissolution as the period of exposure increases irrespective of the concentration of AgNPs. The suitability of nanoparticles as an inhibitor of carbon steel and aluminium corrosion in an acidic environment can be affirmed in this research due to the good inhibition characteristics exhibited by AgNPs on the samples.

Conflict of Interest

The authors proclaim no conflict of interest.

References

[1] Farag AA, 2020. Applications of nanomaterials in corrosion protection coatings and inhibitors. *Corros. Rev.* 38: 67–86. https://doi.org/10.1515/corrrev-2019-0011

[2] ASM International, 2000. The effects and economic impact of corrosion. in: Corrosion: Understanding the basics. *ASM International*, pp 1–20

[3] Anwer KE, Farag AA, Mohamed EA, Azmy EM, Sayedet GH, 2021. Corrosion inhibition performance and computational studies of pyridine and pyran derivatives for API X-65 steel in 6 M H_2SO_4. *J. Ind. Eng. Chem.* 97: 523–538. https://doi.org/10.1016/

j.jiec.2021.03.016

[4] Farag AA, Noor El-Din MR, 2012. The adsorption and corrosion inhibition of some nonionic surfactants on API X65 steel surface in hydrochloric acid. *Corros. Sci.* 64:174–183. https://doi.org/10.1016/j.corsci.2012.07.016

[5] Solomon MM, Gerengi H, Kaya T, Umoren SA, 2017. Performance evaluation of a Chitosan/Silver nanoparticles composite on St37 steel corrosion in a 15% HCl solution. *ACS. Sustain. Chem. Eng.* 5: 809–820. https://doi.org/10.1021/acssuschemeng.6b02141

[6] Saji VS, Thomas J, 2007. Nanomaterials for corrosion control. *Curr. Sci.* 92: 51–55.

[7] Scully JR, Inman SB, Gerard AY, Taylor CD, Windl W, Schreiber DK, Lu P, Saal JE, Frankel GS, 2020. Controlling the corrosion resistance of multi-principal element alloys. *Scr. Mater.* 188: 96–101. https://doi.org/10.1016/j.scriptamat.2020.06.065

[8] Milagre MX, Donatus U, Machado CSC, Araujo JVS, da Silva RMP, de Viveiros BVG, Astarita A, Costa I, 2019. Comparison of the corrosion resistance of an Al–Cu alloy and an Al–Cu–Li alloy. *Corros. Eng. Sci. Technol.* 54: 402–412. https://doi.org/10.1080/1478422X.2019.1605472

[9] Hussain AK, Seetharamaiah N, Pichumani M, Chakra CS, 2021. Research progress in organic zinc rich primer coatings for cathodic protection of metals – A comprehensive review. *Prog. Org. Coatings*, 153:106040. https://doi.org/10.1016/j.porgcoat.2020.106040

[10] Hayatdavoudi H, Rahsepar M, 2017. A mechanistic study of the enhanced cathodic protection performance of graphene-reinforced zinc rich nanocomposite coating for corrosion protection of carbon steel substrate. *J. Alloys Compd.* 727: 1148–1156. https://doi.org/10.1016/j.jallcom.2017.08.250

[11] Odusote JK, Asafa TB, Oseni JG, Adeleke AA, Adediran AA, Yahya RA, Abdul JM, Adedayo SA, 2021. Inhibition efficiency of gold nanoparticles on corrosion of mild steel , stainless steel and aluminium in 1M HCl solution. *Mater. Today Proc.* 38: 578–583. https://doi.org/10.1016/j.matpr.2020.02.984

[12] Asafa T, Odusote J, Ibrahim O, Lateef A, Durowoju MO, Azeez MA, Yekeen TA, Oladipo IC, Adebayo EA, Badmus JA, Sanusi YK, Adedokun O, 2020. Inhibition efficiency of silver nanoparticles solution on corrosion of mild steel , stainless steel and aluminum in 1 . 0 M HCl medium. *IOP. Conf. Ser. Mater. Sci. Eng.* 805: 0–17. https://doi.org/10.1088/1757-899X/805/1/012018

[13] Wang L, Dong C, Man C, Kong D, Xiao K, Li X, 2020. Enhancing the corrosion resistance of selective laser melted 15-5PH martensite stainless steel via heat treatment. *Corros. Sci.* 166:108427. https://doi.org/10.1016/j.corsci.2019.108427

[14] Lindsay R, Lyon SB, 2010. Introduction to control of corrosion by environmental modification. In: *Shreir's Corrosion.* Elsevier, pp 2891–2899

[15] Ahamad I, Prasad R, Quraishi MA, 2010. Thermodynamic, electrochemical and quantum chemical investigation of some Schiff bases as corrosion inhibitors for mild steel in hydrochloric acid solutions. *Corros. Sci.* 52: 933–942. https://doi.org/10.1016/j.corsci.2009.11.016

[16] Atta AM, Allohedan HA, El-Mahdy GA, Ezzat A-RO, 2013. Application of stabilized silver nanoparticles as thin films as corrosion inhibitors for carbon steel alloy in 1 M hydrochloric acid. *J. Nanomater,* 2013:1–8. https://doi.org/10.1155/2013/580607

[17] Kalendová A, Veselý D, Stejskal J, 2008. Organic coatings containing polyaniline and inorganic pigments as corrosion inhibitors. *Prog. Org. Coatings* 62:105–116. https://doi.org/10.1016/j.porgcoat.2007.10.001

[18] Refaey SAM, 2005. Inhibition of steel pitting corrosion in HCl by some inorganic anions. *Appl. Surf. Sci.* 240: 396–404. https://doi.org/10.1016/j.apsusc.2004.07.014

[19] Zheng S, Li J, 2010. Inorganic-organic sol gel hybrid coatings for corrosion protection of metals. *J. Sol-Gel Sci. Technol.* 54:174–187. https://doi.org/10.1007/s10971-010-2173-1

[20] Atta AM, El-Mahdy GA, Al-Lohedan HA, 2013. Corrosion inhibition efficiency of modified silver nanoparticles for carbon steel in 1 M HCL. *Int. J. Electrochem. Sci.* 8:4873–4885.

[21] Izionworu V, Ukpaka C, Oguzie E, 2020. Green and eco-benign corrosion inhibition agents: alternatives and options to chemical based toxic corrosion inhibitors. *Chem. Int.* 6:232–259.

[22] Sharma UR, Sharma N, 2021. Green synthesis, anti-cancer and corrosion inhibition activity of Cr_2O_3 nanoparticles. *Biointerface Res. Appl. Chem.* 11: 8402–8412. https://doi.org/10.33263/BRIAC111.84028412

[23] Alrefaee SH, Rhee KY, Verma C, Quraishi MA, Ebenso EE, 2021. Challenges and advantages of using plant extract as inhibitors in modern corrosion inhibition systems: Recent advancements. *J. Mol. Liq.* 321:114666. https://doi.org/10.1016/j.molliq.2020.114666

[24] Narenkumar J, Parthipan P, Madhavan J, Murugan K, Marpu SB, Suresh AK, Rajasekar A, 2018. Bio-engineered silver nanoparticles as potent anti-corrosive inhibitor for mild steel in cooling towers. *Environ. Sci. Pollut. Res.* 25: 5412–5420. https://doi.org/10.1007/s11356-017-0768-6

[25] Lateef A, Ojo SA, Azeez MA, Asafa TB, Yekeen TA, Akinboro A, Oladipo IC, Gueguim-Kana EB, Beukes LS, 2016. Cobweb as novel biomaterial for the green and eco-friendly synthesis of silver nanoparticles. *Appl. Nanosci.* 6: 863–874. https://doi.org/10.1007/s13204-015-0492-9

[26] Lateef A, Azeez MA, Asafa TB, Yekeen TA, Akinboro A, Oladipo IC, Ajetomobi FE, Gueguim-Kana EB, Beukes LS, 2015. Cola nitida-mediated biogenic synthesis of silver nanoparticles using seed and seed shell extracts and evaluation of antibacterial activities. *Bionanoscience* 5:. https://doi.org/10.1007/s12668-015-0181-x

[27] Zhang S, Liang X, Gadd GM, Zhao Q, 2021. A sol–gel based silver nanoparticle/polytetrafluorethylene (AgNP/PTFE) coating with enhanced antibacterial and anti-corrosive properties. *Appl. Surf. Sci.* 535:147675. https://doi.org/10.1016/j.apsusc.2020.147675

[28] Odusote JK, Ajayi OM, 2013. Corrosion inhibition of mild steel in acidic medium by jathropha curcas leaves extract. *J. Electrochem. Sci. Technol.* 4:81–

87. https://doi.org/10.5229/jecst.2013.4.2.81
[29] Orwa C, Mutua A, Kindt R, Jamnadass R, Simons A, 2009. Agroforestree Database: A tree reference and selection guide, version 4.0. World Agroforestry Centre ICRAF, Nairobi, KE.
[30] Gupta NK, Gopal CSA, Srivastava V, Quraishi MA, 2017. Application of expired drugs in corrosion inhibition of mild steel. *Int. J. Pharm. Chem. Anal.* 4:8–12.
[31] Panossian Z, de Almeida NL, de Sousa RMF, Pimenta GS, Marques LBS, 2012. Corrosion of carbon steel pipes and tanks by concentrated sulfuric acid: A review. *Corros. Sci.* 58:1–11. https://doi.org/10.1016/j.corsci.2012.01.025
[32] Vidales-Herrera J, López I, 2020. Nanomaterials in coatings: An industrial point of view. In: Handbook of Nanomaterials for Manufacturing Applications. *Micro and Nano Technologies*, Elsevier, 51–77.
[33] Islam T, Rashed, HMMA, 2019. Classification and application of plain carbon steels. In Reference Module in Materials Science and Materials Engineering. Elsevier, 1-14.
[34] Vargel C, 2020. 1XXX Series. In Corrosion of Aluminium, Elsevier, 447–451.